

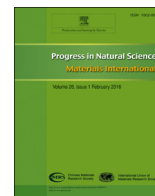
HOSTED BY



ELSEVIER

Contents lists available at [ScienceDirect](http://ScienceDirect)

## Progress in Natural Science: Materials International

journal homepage: [www.elsevier.com/locate/pnsmi](http://www.elsevier.com/locate/pnsmi)

## Original Research

Fabrication of a TiO<sub>2</sub>-P25/(TiO<sub>2</sub>-P25 + TiO<sub>2</sub> nanotubes) junction for dye sensitized solar cellsNguyen Huy Hao<sup>a</sup>, Gobinda Gyawali<sup>a</sup>, Tohru Sekino<sup>b</sup>, Soo Wahn Lee<sup>c,\*</sup><sup>a</sup> Research Center for Eco-multifunctional Nano Materials, Sun Moon University, Asan, Republic of Korea<sup>b</sup> The Institute of Scientific and Industrial Research (ISIR-SANKEN), Osaka University, Japan<sup>c</sup> Department of Environmental and Bio-chemical Engineering, Sun Moon University, Asan, Republic of Korea

## ARTICLE INFO

## Article history:

Received 16 March 2016

Received in revised form

27 July 2016

Accepted 28 July 2016

Available online 10 August 2016

## Keywords:

TiO<sub>2</sub> nanotube

Hydrothermal method

DSSC

Efficiency

Double layer

## ABSTRACT

The dye sensitized solar cell (DSSC), which converts solar light into electric energy, is expected to be a promising renewable energy source for today's world. In this work, dye sensitized solar cells, one containing a single layer and one containing a double layer, were fabricated. In the double layer DSSC structure, the under-layer was TiO<sub>2</sub>-P25 film, and the top layer consisted of a mixture of TiO<sub>2</sub>-P25 and TiO<sub>2</sub> nanotubes. The results indicated that the efficiency of the DSSC with the double layer structure was a significant improvement in comparison to the DSSC consisting of only a single film layer. The addition of TiO<sub>2</sub>-P25 in the top layer caused an improvement in the adsorption of dye molecules on the film rather than on the TiO<sub>2</sub> nanotubes only. The presence of the TiO<sub>2</sub> nanotubes together with TiO<sub>2</sub>-P25 in the top layer revealed the enhancement in harvesting the incident light and an improvement of electron transport through the film.

© 2016 Published by Chinese Materials Research Society. This is an open access article under the CC BY-NC-ND license (<http://creativecommons.org/licenses/by-nc-nd/4.0/>).

## 1. Introduction

In recent years, the depletion of fossil fuels has become one of the big challenges that people are currently facing [1]. This puts great pressure on scientists to find alternative forms of energy. Besides, the overconsumption of the natural energy resources, including fossil fuels, coal, natural oil and natural gas, often causes a detrimental impact on the environment. This is because, as these energy resources are burnt, they release various harmful gases, such as CO, CO<sub>2</sub>, NO<sub>2</sub> and SO<sub>2</sub>, into the atmosphere [2,3]. Consequently, these gases can cause direct damage to the environment, such as through global warming or acid rain [2–4]. Thus, it is necessary to find clean and renewable energy sources which reduce the risks of damage to the natural environment.

These days, the solar cell, which is an electrical device to convert solar energy into electrical energy, has been receiving much attention in research communities. Solar cells convert solar light directly into electric energy without requiring any fuel. Therefore, they avoid the problems of transporting fuel or storing radioactive waste [5]. Hence, these new devices should be studied, developed and applied more widely to replace the use of the conventional sources of energy.

The dye-sensitized solar cell (DSSC) is a type of solar cell which

was reported by Gratzel et al. in 1991 [6]. Basically, a TiO<sub>2</sub>-based DSSC consists of a TiO<sub>2</sub> film layer deposited onto a transparent conductive oxide layer of Fluorine Doped Tin Oxide (FTO), a monolayer of sensitive dye molecules adsorbed on the surface of TiO<sub>2</sub>, redox electrolyte and a counter electrode [7–9]. One of the most important components of a dye sensitized solar cell is the TiO<sub>2</sub> film [10], so there are numerous research projects being carried out which are expected to enhance the power conversion efficiency of solar cells based on TiO<sub>2</sub> film. Lee et al. [11] fabricated TiO<sub>2</sub> film made from the mixture of TiO<sub>2</sub> nanoparticles and nanotubes. The results indicated the effects of the TiO<sub>2</sub> nanotubes in improving the efficiency of DSSC (4.57%) in comparison to nanoparticle film (3.84%) or to the TiO<sub>2</sub> nanotube film (2.49%) only. In the research of Xu et al. [12], a double layer film with TiO<sub>2</sub> nanoparticles as the under-layer and the TiO<sub>2</sub> nanotubes as the upper-layer was fabricated. The results showed that the efficiency of the DSSC made of a double layer was significantly higher (6.15%) than that of a single particle layer (4.25%) or the single nanotube layer (0.37%). According to these research reports, the DSSCs based on a double layer had lower transfer resistance and a longer electron lifetime, leading to improving the performance of the solar cell.

In this work, a dye sensitized solar cell with a double layer junction structure was fabricated. The under-layer was synthesized by TiO<sub>2</sub>-P25. The top layer, in this research, consisted of a mixture of TiO<sub>2</sub>-P25 and TiO<sub>2</sub> nanotubes. The addition of TiO<sub>2</sub>-P25 in the top layer was made to improve the adsorption of the sensitized dye on the film, since TiO<sub>2</sub>-P25 reveals a higher level of dye

\* Corresponding author.

E-mail address: [swlee@sunmoon.ac.kr](mailto:swlee@sunmoon.ac.kr) (S.W. Lee).

adsorption than the TiO<sub>2</sub> nanotubes film [13]. Also, the use of TiO<sub>2</sub> nanotubes might enhance the incident light harvest and improve electron transport through the film as well. These changes are expected to improve the efficiency of the solar cell.

## 2. Experimental procedure

### 2.1. Preparation of the TiO<sub>2</sub> nanotubes

In this research, the TiO<sub>2</sub> nanotubes were synthesized by the microwave-assisted hydrothermal method. The synthesis process followed the method given by Cho et al. [14,15]. The precursors used to prepare the TNTs were TiO<sub>2</sub>-P25 Degussa and Sodium Hydroxide (98% purity, Samchun Chemical), and these chemicals were used without further purification. Firstly, 2 g of TiO<sub>2</sub>-P25 was added into 100 ml of 10 M NaOH aqueous solution under through by stirring at room temperature for 15 min to form a suspension. After that, this suspension was transferred into a Teflon vessel reactor to begin the microwave-assisted hydrothermal reaction at 150 °C, 195 W and a rotation speed of 300 rpm for 4 h. The pH of the suspension obtained after this hydrothermal process was adjusted to 7 with 5 N HCl aqueous solution [14]. And then, the resulting product was repetitively washed with distilled water and centrifuged to eliminate residual NaCl. Finally, the synthesized sample was dried in a freeze dryer (EYELA, FDU-2100) for 24 h at –80 °C.

### 2.2. Synthesis of the TiO<sub>2</sub> paste

The TiO<sub>2</sub> paste was prepared following the method given by Ito et al. [16]. In the first step, a 1 g TiO<sub>2</sub> nanotube prepared as above was taken out and put in a mortar, and 0.17 ml acetic acid was then added drop by drop into the TiO<sub>2</sub> nanotubes, followed by grinding for 5 min at room temperature. In the second step, 0.17 ml distilled water was added into the mortar, and the mixture was ground for 1 min. This process was then repeated 5 times. The third step was conducted with the same process as the second step, however, this step used ethanol instead of distilled water, and it was repeated 15 times. In the next step, 0.42 ml ethanol was dropped into the mixture, and then the mixture was ground for 1 min. This step was repeated 6 times. Next, the TiO<sub>2</sub> paste was transferred into a beaker and 16.7 ml ethanol was added. Then, the mixture was subjected to magnetic stirring for 1 min, and ultrasonically homogenized for 2 min. Following this step, 3.33 g  $\alpha$ -

terpineol was added into the paste, and the TiO<sub>2</sub> paste then continued to be magnetically stirred for 1 min and underwent the ultrasonic treatment for 2 min. Next, a 5 g ethyl cellulose solution (10%) was dropped into the mixture, and the mixture received the ultrasonic treatment for 2 min and magnetic stirring for 1 min. Finally, the mixture was evaporated to remove the residual ethanol.

### 2.3. Fabrication of DSSCs

Three different TiO<sub>2</sub> photoanode films, corresponding to the TiO<sub>2</sub> nanotubes (sample 1), TiO<sub>2</sub>-P25 (sample 2) and TiO<sub>2</sub> P25/ (mixture of 90% P25 and 10% TNT) (sample 3), were fabricated following the doctor-blade method. After coating the TiO<sub>2</sub> pastes on the FTO glass, the electrodes were heated at 125 °C for 5 min, at 325 °C for 5 min and at 450 °C for 30 min. In the case of the double layer, the underlayer was deposited first, and then this under film was dried at 125 °C for 5 min before coating the top layer. This double layer was also treated with the heating process above. The TiO<sub>2</sub> films were then immersed in a 90 mM TiCl<sub>4</sub> solution at 70 °C for 30 min and sintered again at 450 °C for 30 min [16]. When the temperature of the electrodes decreased to 90 °C, they were immersed into a 0.6 mM N-719 dye solution for 24 h [17]. Finally, the TiO<sub>2</sub> electrode was assembled with a Pt-counter electrode to form a dye sensitized solar cell. The active area of the resulting cell exposed to light was approximately 0.25 cm<sup>2</sup>.

### 2.4. Characterization of DSSCs

The crystal structure of all samples was analyzed by X-ray diffraction (XRD, RINT-2200, Rigaku) patterns from 5° to 70° using a monochromatized Cu-K $\alpha$  ( $\lambda$ =1.54 Å) radiation. The microstructure of the TiO<sub>2</sub> nanotubes was observed by transmission electron microscopy (TEM, JEM-2100F, Jeol). The thickness of the TiO<sub>2</sub> layer film was examined with scanning electron microscope (SEM, JEOL-2020). The conversion efficiency of the fabricated DSSC was measured under a simulated solar light source (Portable solar simulator PEC-L01, Pecell 200 W) (Am 1.5G). Electrochemical Impedance (EIS) and Incident Photon Conversion Efficiency (IPCE) were measured by IVIUMSTAT (electrochemical interface, Netherlands).

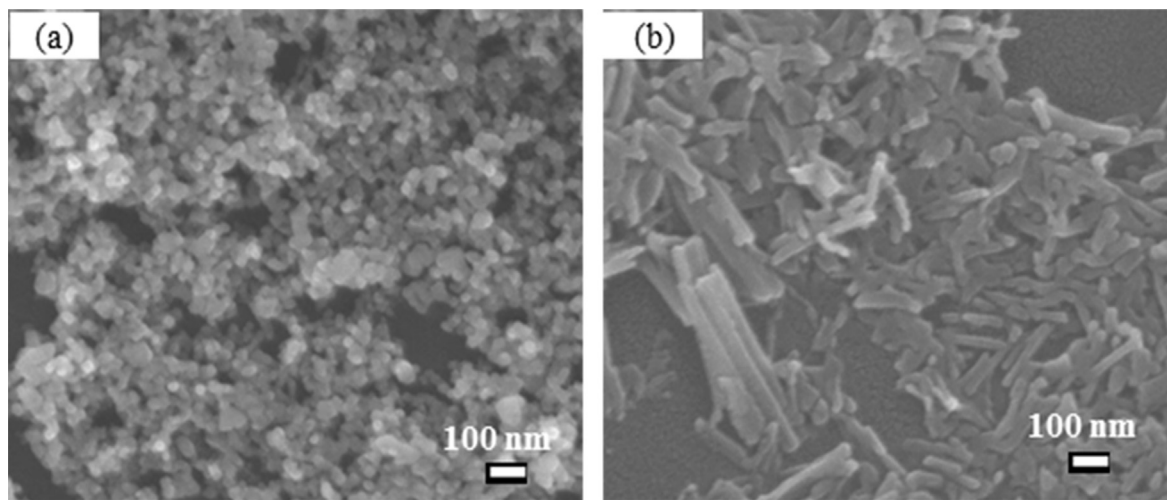


Fig. 1. FESEM images of the samples: (a) TiO<sub>2</sub>-P25, and (b) TiO<sub>2</sub> nanotubes.

### 3. Results and discussion

The FE-SEM images of  $\text{TiO}_2$ -P25 and the synthesized  $\text{TiO}_2$  nanotubes are shown in Fig. 1. It can be seen that the  $\text{TiO}_2$ -P25 (Fig. 1a) completely transformed into  $\text{TiO}_2$  nanostructures (Fig. 1b). Further TEM investigation was performed in order to determine the actual nanostructure formed. The TEM image (as shown in Fig. 2) confirms the nanotube structure of the  $\text{TiO}_2$ . It is clearly observed in the TEM image that the  $\text{TiO}_2$  nanotubes were formed with an average length of around 100 nm and a diameter of 8 nm, respectively. Fig. 3 shows the XRD patterns of the  $\text{TiO}_2$ -P25 precursor and the synthesized TNT sample. It can be seen that the  $\text{TiO}_2$ -P25 consists of the rutile and anatase phase with a higher level of crystallinity. However, the degree of crystallinity of the synthesized  $\text{TiO}_2$  nanotubes is very low, and the TNT sample has four main peaks, at around  $9^\circ$ ,  $24.3^\circ$ ,  $28.4^\circ$ , and  $48.3^\circ$ . According to the literature [18,19], these peaks reveal the layered titanates of  $\text{TiO}_2$  nanotubes. The thickness of the  $\text{TiO}_2$  film double layer in the dye sensitized solar cell is shown in Fig. 4. It is about  $27\ \mu\text{m}$  thick, and the same thickness was made for all samples.

Fig. 5 shows the incident photon to current conversion efficiency (IPCE) spectra of the three different dye sensitized solar cells. The IPCE spectra provide further evidence of the light harvesting efficiency of the DSSCs. As can be seen, a maximum IPCE of all the samples at 530 nm is about 28% (100% TNT), 38% (100% P25) and 94% (double layer), corresponding to the absorption peak of the N719 dye. The DSSC fabricated from double layers displays the highest IPCE value over a wide range in the visible light area, from 400 nm to 700 nm, among these solar cells. The higher IPCE of the double layer sample in comparison with the single layer of the  $\text{TiO}_2$  nanotube or the  $\text{TiO}_2$ -P25 indicated the significant impact of the TNT on the solar cell.

The efficiency, short circuit current ( $I_{\text{sc}}$ ), short circuit current density ( $J_{\text{sc}}$ ), open circuit voltage ( $V_{\text{oc}}$ ), and the fill factor (ff) of the precursor  $\text{TiO}_2$ -P25, the TNT, and the P25/TNT junctions for the solar cells are summarized in Fig. 6 and Table 1. The data indicated that the  $V_{\text{oc}}$  and fill factor values of the DSSCs based on the three films have no significant changes. It can be seen that, there are slight variations in the values of the current density of sample 1 (TNT film) and sample 2 (P25 film), corresponding to 7.648 ( $\text{mA}/\text{cm}^2$ ) and 9.504 ( $\text{mA}/\text{cm}^2$ ). However, this figure increased to 16.380 ( $\text{mA}/\text{cm}^2$ ) for the photoanode of P25/(a mixture of 90% P25 and 10% TNT). This leads to the higher efficiency of sample 3 (6.862%), which is greater than that of sample 1 (3.646%) and sample 2 (4.435%). The better performances of sample 2 as compared to sample 1 might be explained by the larger amount of dye molecules adsorbed on the  $\text{TiO}_2$  film [20]. For sample 3, a small

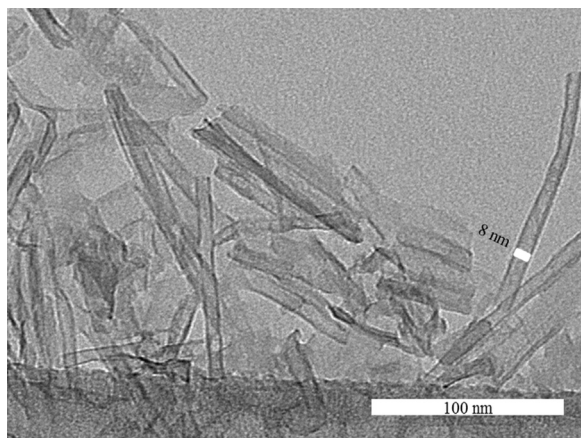


Fig. 2. TEM images of the  $\text{TiO}_2$  nanotubes.

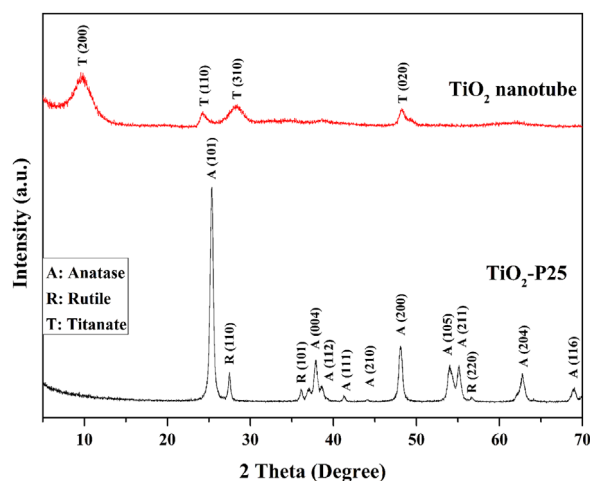


Fig. 3. XRD patterns of the  $\text{TiO}_2$ -P25 and  $\text{TiO}_2$  nanotubes.

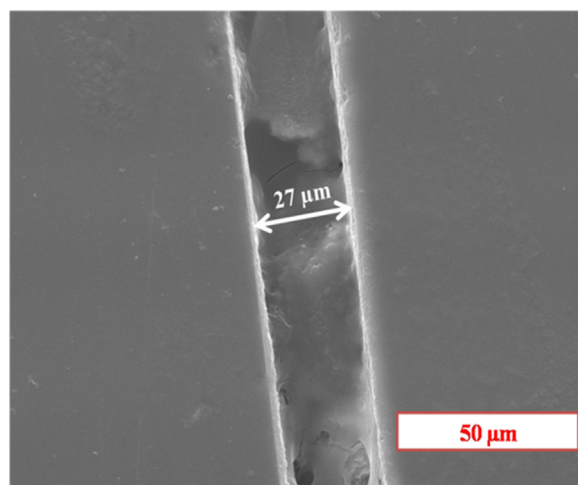


Fig. 4. The thickness of the  $\text{TiO}_2$  double layer in the DSSC.

amount of TNT in the main layer P25, which contributes to a significant increase in DSSCs performance in sample 3 as compared to the other samples, can be explained on the basis of the electrochemical impedance analysis.

Electrochemical impedance spectroscopy (EIS) is a powerful tool used to clearly analyze the charge transfer resistance in DSSCs [21]. Fig. 7 and Table 2 show the EIS results of the DSSCs. It is seen that  $R_{\text{ct}}$ , which is represented to electron transfer resistance at the interface between the  $\text{TiO}_2$ /dye/electrolyte of sample 1 (TNT film), has a smaller value than sample 2 (P25 film). This result indicates that the electron transport through nanotubes is easier than through  $\text{TiO}_2$ -P25. Therefore, the film layer of sample 3 included with the  $\text{TiO}_2$ -P25 and  $\text{TiO}_2$  nanotubes will benefit both dye adsorption and electron transport. Furthermore, the charge transfer resistance ( $R_{\text{pt}}$ ) is lower in sample 3, which enhances the performance of the solar cell. The impact of these factors leads to the higher efficiency of sample 3 compared to the others.

The results of the current density, IPCE and EIS of the sample 3 are more beneficial to explain the role of TNT in the double layer to enhance the efficiency of DSSCs. In the structure of the electrode layer, a mixture of the  $\text{TiO}_2$  nanotubes and  $\text{TiO}_2$ -P25 considerably impacts the performance of the DSSCs. This is because if the film layer contains only the large size particles, like  $\text{TiO}_2$  nanotubes (sample 1), the surface per unit volume may decrease. Consequently, the amount of dye adsorbed on the  $\text{TiO}_2$  film becomes very small [22]. On the other hand, there are several



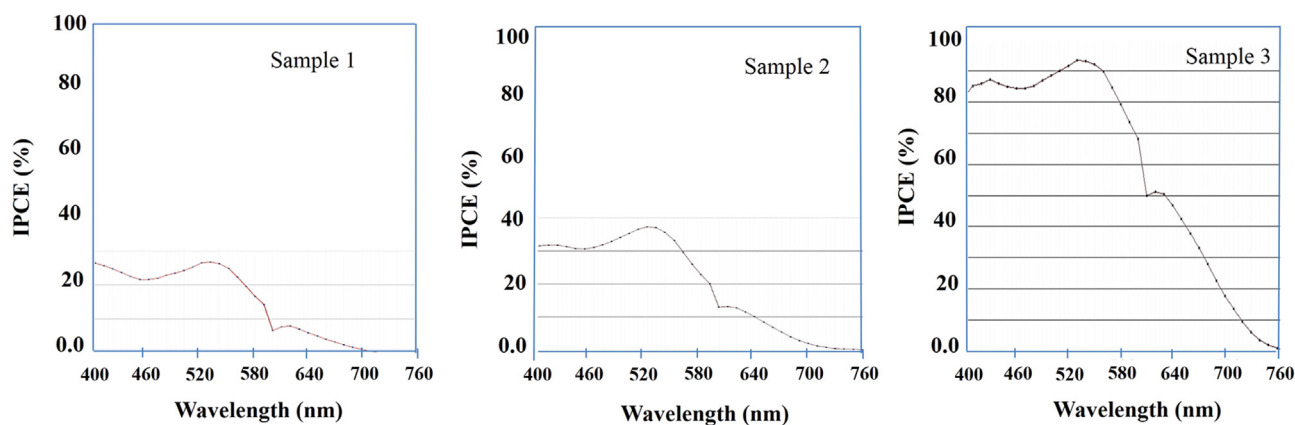


Fig. 5. IPCE spectra of sample 1 (TNT), sample 2 (TiO<sub>2</sub>-P25), and sample 3 (P25/(P25-TNT junction)).

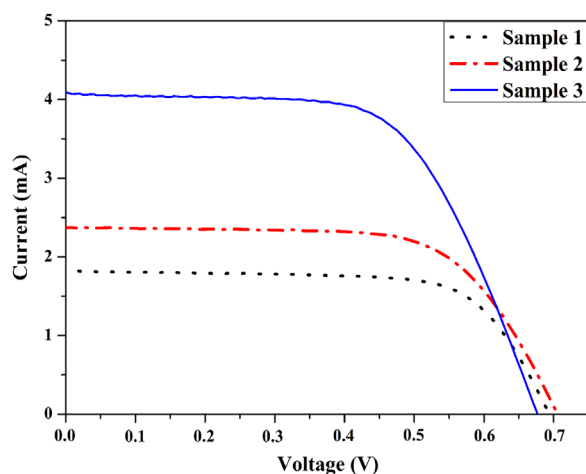


Fig. 6. The photocurrent-voltage curve of the DSSCs made by sample 1 (TNT), sample 2 (TiO<sub>2</sub>-P25), and sample 3 (P25/(P25-TNT junction)).

**Table 1**  
Photovoltaic parameters of DSSCs.

Samples	V <sub>oc</sub> (V)	I <sub>sc</sub> (mA)	J <sub>sc</sub> (mA/cm <sup>2</sup> )	Fill factor	Efficiency (%)
Sample 1 (100% TNT)	0.690	1.912	7.648	0.690	3.646
Sample 2 (100% P25)	0.705	2.376	9.504	0.619	4.435
Sample 3 (P25/(P25-TNT))	0.675	4.095	16.380	0.620	6.862

disadvantages of the film layer consisting of only small particles such as TiO<sub>2</sub>-P25 (sample 2). Firstly, a number of small-sized nanoparticles might increase the grain boundaries. As a result, a large number of electron trapping sites are formed [22]. Secondly, smaller TiO<sub>2</sub> particles can prevent the penetration of the dye molecules and electrolytes into the inner TiO<sub>2</sub> layer [22]. In our study, a junction between the TiO<sub>2</sub>-P25 and TiO<sub>2</sub>-P25/TNT mixture, was created to enhance the level of dye adsorption in the double layer structure as compared to the single layer film. Similarly, this double layer film can facilitate the movement of dye molecules and electrolytes. Furthermore, it can also decrease the grain boundaries of the double layer electrode film. As a result, the presence of TiO<sub>2</sub> nanotubes in the double layer film causes to improve the incident light harvesting and the electron transport through the TiO<sub>2</sub> layer. Consequently, the enhancement in IPCE and short-circuit current density (J<sub>sc</sub>) were observed. The results of electrochemical impedance spectroscopy (EIS) of the samples

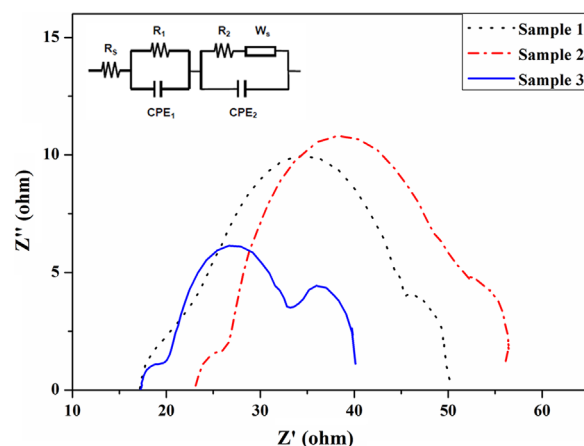


Fig. 7. Electrochemical impedance spectra (EIS) of sample 1 (TNT), sample 2 (TiO<sub>2</sub>-P25), and sample 3 (P25/(P25-TNT junction)).

**Table 2**  
Series resistance (R<sub>s</sub>), charge transfer resistance (R<sub>pt</sub>) and electron transfer and recombination (R<sub>ct</sub>) of the DSSCs.

Samples	R <sub>s</sub> /Ω	R <sub>pt</sub> /Ω	R <sub>ct</sub> /Ω
Sample 1 (100% TNT)	15.63	33.45	4.265
Sample 2 (100% P25)	17.46	23.64	4.95
Sample 3 (P25/(P25-TNT))	17.15	18.23	2.97

demonstrated more clearly the key function of the TiO<sub>2</sub> nanotubes in the top layer. The efficient electron transfer at the interface between the TiO<sub>2</sub>/dye/electrolyte (represented by R<sub>ct</sub>) of sample 3 (a mixture of TNT and P25), rather than that of sample 1 (100% TNT) and sample 2 (100% P25), be explained as follows: for sample 1 (100% TNT), the large size of the nanotubes may create many interlocked spaces between the nanotubular TiO<sub>2</sub>, which results in deterring the transport of electrons. Consequently, the photocurrent will decrease and negatively affect the efficiency of the solar cell. For sample 2 (100% P25), due to the smaller size of the particles, a large number of the TiO<sub>2</sub> particles can occupy the allocated space, and that leads to an enhancement of the level of dye adsorption on the TiO<sub>2</sub> layer. However, the smaller size causes an increase in the border of the particles and accelerates the charge recombination rate. This contributed to a decrease in the efficiency of DSSC. The data from EIS are suitable for the above explanation of IPCE. Therefore, the mixture of the TiO<sub>2</sub> particles and TiO<sub>2</sub> nanotubes can be beneficial to the performance of solar cells.

In the previous literature, Lee et al. [11] and Xu [12] also fabricated dye sensitized solar cells, which consisted of a double layer.

The under-layer with TiO<sub>2</sub> particles [11] and TiO<sub>2</sub>-P25 [12], and the top layer, contained TiO<sub>2</sub> nanotubes, respectively. However, the best efficiency obtained was only 4.57% [11] and 6.15% [12], respectively, which is lower than the efficiency shown by this study. These reference efficiencies are significant, and are practical evidence which may contribute to understanding more clearly the utmost importance of TNT in the top layer.

#### 4. Conclusion

In this study, the important role of the TiO<sub>2</sub> nanotubes in DSSCs was clarified. It was found that the conversion efficiency of DSSCs was positively impacted by the combination of TiO<sub>2</sub> nanoparticles and TiO<sub>2</sub> nanotubes. The dye sensitized solar cells fabricated by the TiO<sub>2</sub> nanoparticles in the under-layer, and the mixture of the TiO<sub>2</sub> nanoparticles and the TiO<sub>2</sub> nanotubes in the upper-layer indicated a better performance than the DSSCs made either by only pure nanoparticles or only by nanotubes.

#### Acknowledgments

This research was supported by the Global Research Laboratory Program of the National Research Foundation of Korea (NRF) funded by the Ministry of Education, Science and Technology (MEST) of Korea (Grant number: 2010-00339).

#### References

- [1] M. Asif, T. Muneer, *Renew. Sustain. Energy Rev.* 11 (2007) 1388–1413.
- [2] Natgas, (<http://naturalgas.org/environment/naturalgas/>).
- [3] D. Sengupta, P. Dasa, B. Mondala, K. Mukherjee, *Renew. Sustain. Energy Rev.* 60 (2016) 356–376.
- [4] ([http://www.ucsusa.org/clean\\_energy/our-energy-choices/coal-and-other-fossil-fuels/the-hidden-cost-of-fossil.html#.Vujl4dJ967A](http://www.ucsusa.org/clean_energy/our-energy-choices/coal-and-other-fossil-fuels/the-hidden-cost-of-fossil.html#.Vujl4dJ967A)).
- [5] Y. Alivov, Z.Y. Fan, *Appl. Phys. Lett.* 95 (2009) 063504.
- [6] B. O'Regan, M. Gratzel, *Nature* 353 (1991) 737–740.
- [7] L. Han, A. Islam, H. Chen, C. Malapaka, B. Chiranjeevi, S. Zhang, X. Yang, M. Yanagida, *Energy Environ. Sci.* 5 (2012) 6057–6060.
- [8] K.H. Park, T.Y. Kim, J.H. Kim, H.J. Kim, C.K. Hong, J.W. Lee, *J. Electroanal. Chem.* 708 (2013) 39–45.
- [9] P. Roy, D. Kim, K. Lee, E. Spiecker, P. Schmuki, *Nanoscale* 2 (2010) 45–49.
- [10] F.O. Lenzmann, J.M. Kroon, *Adv. Optoelectron.* 2007 (2007) 65073.
- [11] C.H. Lee, S.W. Rhee, H.W. Choi, *Nanoscale Res. Lett.* 7 (2012) 48.
- [12] H. Xu, X. Tao, D.T. Wang, Y.Z. Zheng, J.F. Chen, *Electrochim. Acta* 55 (2010) 2280–2285.
- [13] M. Adachi, Y. Murata, J. Takao, J. Jiu, M. Sakamoto, F. Wang, *J. Am. Chem. Soc.* 126 (2004) 14943–14949.
- [14] S.H. Cho, G. Gyawali, R. Adhikari, T.H. Kim, S.W. Lee, *Mater. Chem. Phys.* 145 (2014) 297–303.
- [15] S.H. Cho, H.H. Nguyen, G. Gyawali, S.J. Eun, T. Sekino, B. Joshi, S.H. Kim, Y.H. Jo, T.H. Kim, S.W. Lee, *Catal. Today* 266 (2016) 46–52.
- [16] S. Ito, P. Chen, P. Comte, M.K. Nazeeruddin, P. Liska, P. Péchy, M. Grätzel, *Progress in Photovolt.* 15 (2007) 603–612.
- [17] J.H. Yang, C.W. Bark, K.H. Kim, H.W. Choi, *Materials* 7 (2014) 3522–3532.
- [18] C.K. Lee, C.C. Wang, M.D. Lyu, L.C. Juang, S.S. Liu, S.H. Hung, *J. Colloid Interface Sci.* 316 (2007) 562–569.
- [19] J. Yang, Z. Jin, X. Wang, W. Li, J. Zhang, S. Zhang, X. Guo, Z. Zhang, *Dalton Trans.* 20 (2003) 3898–3901.
- [20] X. Wu, Q.Z. Jiang, Z.F. Ma, M. Fu, W.F. Shangguan, *Sol. Stat. Commun.* 136 (2005) 513–517.
- [21] S. Sarker, A.J. Ahammad, H.W. Seo, D.M. Kim, *Int. J. Photo.* 2014 (2014) 851705.
- [22] K. Basu, D. Benetti, H. Zhao, L. Jin, F. Vetrone, A. Vomiero, F. Rosei, *Sci. Rep.* 6 (2016) 23312.